

Published in final edited form as:

Nat Cancer. 2023 April 01; 4(4): 454–467. doi:10.1038/s43018-023-00526-x.

Single-cell profiling to explore pancreatic cancer heterogeneity, plasticity and response to therapy

Stefanie Bärthel^{1,2,3}, **Chiara Falcomatà**^{1,2,3,4}, **Roland Rad**^{3,5,6}, **Fabian J. Theis**^{7,8}, **Dieter Saur**^{1,2,3,*}

¹Division of Translational Cancer Research, German Cancer Research Center (DKFZ) and German Cancer Consortium (DKTK), Im Neuenheimer Feld 280, 69120 Heidelberg, Germany

²Chair of Translational Cancer Research and Institute of Experimental Cancer Therapy, Klinikum rechts der Isar, School of Medicine, Technische Universität München, Ismaninger Str. 22, 81675 Munich, Germany

³Center for Translational Cancer Research (TranslaTUM), School of Medicine, Technical University of Munich, Ismaninger Str. 22, 81675 Munich, Germany

⁴Precision Immunology Institute, Icahn School of Medicine at Mount Sinai, New York, NY, USA

⁵Institute of Molecular Oncology and Functional Genomics, School of Medicine, Technische Universität München, 81675 Munich, Germany

⁶German Cancer Consortium (DKTK), Im Neuenheimer Feld 280, 69120 Heidelberg, Germany

⁷Institute of Computational Biology, Helmholtz Zentrum München - German Research Center for Environmental Health, Neuherberg, Germany

⁸Department of Mathematics, Technical University of Munich, Munich, Germany

Abstract

Pancreatic ductal adenocarcinoma (PDAC) is a highly lethal cancer entity characterized by a heterogeneous genetic landscape and an immunosuppressive tumor microenvironment. Recent advances in high-resolution single-cell sequencing and Spatial Transcriptomics technologies have enabled an in-depth characterization of both malignant and host cell types and increased our understanding of the heterogeneity and plasticity of PDAC in steady-state and under therapeutic perturbation. In this review, we outline single-cell analyses in PDAC, discuss their implications on our understanding of the disease and present future perspectives of multimodal approaches to elucidate its biology and response to therapy at the single-cell level.

*Correspondence: Dieter Saur, Tel. +49-89-4140-5255, Fax. +49-89-4140-7289, dieter.saur@tum.de.

Author contributions

S.B., C.F., R.R., F.J.T. and D.S. wrote the paper.

Competing Interests

F.J.T. consults for Immunai Inc., Singularity Bio B.V., CytoReason Ltd, Cellarity and Omniscope Ltd, and has an ownership interest in Dermagnostix GmbH and Cellarity. The other authors declare no competing interests.

Introduction

Pancreatic ductal adenocarcinoma (PDAC) is a complex disease characterized by a dismal prognosis. The 5-year survival rate of 12% constitutes one of the lowest of all tumor entities¹ and with its incidence on the rise PDAC is projected to become the second leading cause of cancer-related deaths within this decade². There are many reasons for its poor prognosis, including late-stage diagnosis, high aggressiveness (often preventing surgical tumor resection), frequent metastasis formation and primary resistance to all forms of therapies. Large-scale molecular analyses of the PDAC genetic landscape revealed only a few predominant difficult-to-treat driver lesions, namely, mutations in *KRAS*, *TP53*, *CDKN2A* and *SMAD4*, and multiple additional genetic alterations including profound copy number variations at lower frequency, contributing to the genetic diversity of the disease^{3–7}. In addition, PDAC is characterized by an immunosuppressive tumor microenvironment (TME) encompassing a multitude of different cell types⁸. This includes variable numbers of infiltrating immunosuppressive cells, such as tumor-associated macrophages (TAMs), myeloid-derived suppressor cells (MDSCs), regulatory T cells (T_{reg} cells), dysfunctional T cells and distinct cancer-associated fibroblast (CAF) subtypes, as well as a heterogeneous extracellular matrix (ECM) composition, which impact patient prognosis and therapeutic outcome^{8–15}. These features pose a challenge and identify an unmet need for more mechanistic understanding and the identification of novel therapeutic vulnerabilities that can be translated into effective treatment strategies.

Mutationally activated *KRAS* (*KRAS*-mut) drives more than 90% of human PDAC cases^{5,16} and increased oncogenic *KRAS* gene dosage and signaling drive phenotypic diversification, including tumor cell differentiation, metastasis formation and clinical outcome^{5,7,17,18}. Indeed, the most undifferentiated mesenchymal PDAC subtype, characterized by a basal-like gene expression program, high metastatic potential, therapy resistance and worse prognosis, shows the strongest increase in *KRAS* gene dosage^{5,7,17}. In contrast, the gland-forming classical subtype is characterized by an epithelial differentiation state and transcriptional program and displays better treatment responses and prognosis^{5,7,16,19–25}.

Subtype classifications are not only based on tumor cell-intrinsic features but also on differences in immune and stroma characteristics. On the level of morphology, classical gland-forming tumors are typically encompassed by a highly abundant ECM and CAF-rich tumor stroma, whereas basal-like mesenchymal tumors display higher tumor cell cellularity and less ECM deposition^{17,23,26–28}. This implies that PDAC subtypes are capable of shaping their distinct TMEs; however, the underlying mechanisms remain poorly understood^{8,29}.

Historically, PDAC profiling and classification studies used histochemistry and immunohistochemistry, magnetic or fluorescence-activated cell sorting (FACS), CyTOF, *in situ* hybridization and macro- or microdissection of tumor tissue. Transcription based profiling attempts employed bulk RNA sequencing (RNA-seq) approaches followed by bioinformatic deconvolution. Computational microdissection through non-negative matrix factorization or laser capture microdissection of specific cell types has been used to identify distinct tumor and stromal expression signatures^{16,21,30}. While these attempts have uncovered the enormous heterogeneity of PDAC and revealed the existence of unique cancer

cell and TME subtypes with prognostic and therapeutic relevance^{5,8,16,20,25}, the advent of single-cell sequencing-based profiling technologies opened fundamental new avenues to dissect PDAC heterogeneity and plasticity holistically. For example, such analyses, combined with novel lineage tracing and barcoding strategies, are indispensable in the delineation of intermediate states of tumor cells and their potential cellular plasticity, or mixed phenotypes (presence of classical and mesenchymal cancer cells within one tumor), as well as the composition, polarization and communication of cells within the tumor cell-TME niche (Figure 1 and 2).

In this Review, we discuss how single-cell technologies and approaches have revolutionized the PDAC field. First, we focus on key approaches that have enabled deep phenotyping of PDAC and discuss the discovery of important subtypes of the disease, including their immune phenotypes. Furthermore, we examine how standard-of-care chemotherapy and targeted therapies impact PDAC subtypes and phenotypes. Finally, we discuss fundamental open questions and corresponding single-cell approaches, which promise to uncover the drivers of tumor and TME heterogeneity and plasticity, as well as mechanisms of therapeutic response and resistance.

Single-cell profiling to disentangle the complexity of PDAC

Single-cell profiling approaches are powerful methods to unbiasedly investigate the complex biologic ecosystem of PDAC in high-resolution. In particular, droplet-based single-cell RNA-seq (scRNA-seq) analysis has been massively improved over the last decade, leading to the ability to interrogate the transcriptomic profile of thousands (and recently millions) of cells in parallel^{31–33}. Single-cell technologies have evolved rapidly and now encompass a wide spectrum of applications, such as scRNA-seq (transcriptomics), scDNA-seq (genomics and DNA methylation), single-cell sequencing assay for transposase-accessible chromatin (scATAC-seq; epigenetics and chromatin accessibility), proteomics and metabolomics^{34,35}, leveraging multiple stages of the central dogma beyond pure transcriptomics³⁶ (Figure 1 and 2 and Box 1).

Advanced spatial profiling technologies are crucial to resolve the complex tissue architecture of PDAC and the relationships between cells at the single-cell level^{37,38,39} (Figure 2 and 3 and Box1). They provide fundamental insights into the spatial organization of cellular neighborhoods and interactions that for example support tumor growth or mediate immune escape. Spatial transcriptome-profiling technologies for single cells include sequential fluorescent RNA *in situ* hybridization (FISH) approaches, such as MERFISH or seqFISH³⁷. Digital spatial profiling (GeoMx platform) enables transcriptome-wide spatial profiling by simultaneous hybridization of messenger RNA probes in selected regions of interest^{39,40}. Furthermore, spot-based spatial transcriptomics methods assess cells transcriptome wide with the caveat of lower resolution (Visium and Slide-seq assays)⁴¹. Spatially resolved profiling of protein expression is achieved using multiplexed immunofluorescent staining and imaging approaches, such as co-detection by indexing (CODEX), which can visualize up to 100 proteins of interest simultaneously³⁷.

The rapid development of novel high-throughput assays necessitated a whole range of new computational tools and modeling approaches with the aim, among others, of determining cell types, modeling transitions and quantifying differences across conditions, for transcriptomics, multimodal and spatial measurements^{37,42–45}. A particularly relevant, recent direction is data integration across modalities as well as datasets⁴⁶. The latter allows the building of integrated cell-type maps across multiple resources as well as disease conditions, toward the initial lofty goal of single-cell organ atlases, as promised for example by the Human Cell Atlas⁴⁷. These resources, combined with advances in machine learning, now allow the mapping of novel datasets on top of these references^{43,48}, thereby automatically annotating cell types and reflecting differences compared with controls. While this was initially pioneered for single-cell transcriptomics, recent advances allow mapping across modalities and also the imputation of missing modalities^{49–51}.

The recent development of a multitude of highly sophisticated single-cell profiling tools (Figure 1–3 and Box 1) holds great promise and has already provided invaluable novel insights that could not be achieved by other technologies⁵².

Below, we will provide a comprehensive overview of such studies. Selected studies are listed in addition in Table 1.

PDAC heterogeneity and plasticity under steady-state and therapeutic perturbation

Genomic profiling of human and mouse PDAC has provided fundamental insights into its evolution and phenotypic diversification^{5,7,17,18}. Moreover, transcriptomic profiling of bulk and microdissected tumors has revealed molecular subtypes of the disease; for instance, classical and mesenchymal/basal-like PDAC²⁰ (Figure 4). By performing gene expression profiling of laser capture microdissection epithelium from 248 human tumors, followed by non-negative matrix factorization clustering, this classification has been further refined to five subtypes designated as basal-like A, basal-like B, hybrid, classical-A and classical-B. The basal-like subtypes are linked to allelic imbalances of *KRAS*, as previously described in PDAC mouse models^{7,17,18} and the hybrid cluster presents an overlap of basal-like (mesenchymal) and classical gene expression signatures⁷. scRNA-seq of 15 PDAC specimens further uncovered the presence of both the basal-like and classical signature within the same tumor in individual patients, indicating the presence of cells of both subtypes within one tumor⁷.

scRNA-seq of disseminated circulating tumor cells in the peripheral blood, as well as metastatic PDAC cells, revealed an additional intermediate co-expressor cluster, which showed expression of classical and basal signatures in the same cell^{53,54} (Figure 4). PDAC circulating tumor cells were also enriched in stem cell markers and furthermore showed high abundance of ECM genes, such as *SPARC*, pointing to a connection of the ECM to cell states that lead to invasiveness and metastasis formation⁵⁴.

Analysis of intermediate co-expressor cells from metastases demonstrated enrichment of RAS signaling, the inflammatory/stress response and developmental gene sets that might

represent a transitional state between classical and basal-like programs⁵³. Importantly, the three distinct tumor cell clusters (classical, basal-like and intermediate co-expressor) were associated with distinct TME states. Classical and intermediate co-expressor tumors showed a greater TME diversity with infiltration of *SPPI*⁺ macrophages, which are enriched in genes involved in angiogenesis and co-localize with fibroblast activation protein-positive (FAP⁺) fibroblasts, while basal tumors had a lower diversity and were specifically infiltrated by immunosuppressive *CIQC*⁺ macrophages. The intermediate co-expressor state positively correlated with higher T cell infiltration, and particularly with *IFNG* expressing CD8⁺ T cells⁵³.

Subtype classification was not only performed in patient specimens, but also on isolated matching organoids in vitro. Notably, organoids derived from the classical subtype displayed a stable classical state in culture. In contrast, the basal and intermediate co-expressor state could not be propagated in their original subtype and displayed a transition to an organoid-specific or classical state in vitro. Subsequent investigation of paracrine signaling from nonmalignant cells based on the in vivo scRNA-seq dataset revealed TME-derived factors important for subtype specification; for example, transforming growth factor β (TGF β), which leads to a basal-like organoid cell state⁵³. Classical organoids were more sensitive to chemotherapy, reinstating what was observed in previous studies^{6,55}. The subsequent integration of six scRNA-seq datasets of 70 patient samples established a first atlas of the refined subtype classification of classical, basal-like and intermediate malignant cell states of human PDAC⁵⁶.

The advent of single-nucleus RNA-seq (snRNA-seq) in combination with spatial transcriptomics enabled the deep transcriptional and spatial characterization of 18 treatment-naive and 25 neoadjuvant-treated primary PDAC specimens and revealed novel subtypes and their potential plasticity under therapy³⁹ (Figure 4). The majority of treated patients received FOLFIRINOX chemotherapy followed by radiotherapy and continuous fluorouracil/capecitabine treatment. snRNA-seq has the advantage that it can be applied to frozen samples and shows an increased recovery rate of malignant and stromal cell populations, thus overcoming one major limitation of droplet-based scRNA-seq experiments. Profiling of the 43 human PDAC samples delineated several distinct tumor cell lineages partly overlapping with the previously described subtypes. Identified lineage programs include acinar-like (ACN), classical (CLS), basaloid (BSL), squamoid (SQM), mesenchymal (MES), neuroendocrine-like (NEN) and neural-like progenitor (NRP) malignant cell states. Thus, snRNA-seq of treated and untreated PDAC specimens enabled the fine-mapping of cancer cell states and led to a refined classification of PDAC subtypes (Figure 4). This is clinically relevant, because the NEN and NRP programs are enriched, whereas CLS and SQM signatures are decreased, in patients after neoadjuvant treatment, indicating therapy-mediated lineage program induction and/or selection. Importantly, the NRP program is also associated with a poor prognosis in patients with PDAC. Mechanisms by which NRP malignant cells might mediate treatment resistance remain elusive but are potentially governed by NRP transcriptional program genes (e.g., *ABC11*, *BCL2*, *PDGFD* and *SPPI*) having a role in negative regulation of cell death, chemoresistance and drug efflux, as well as neuronal migration, axon guidance and tumor-nerve crosstalk³⁹.

Integration of digital spatial gene expression profiling and snRNA-seq datasets allowed the linkage of these malignant programs with TME features and their spatially resolved distribution³⁹. Thereby, three multicellular communities were identified—namely, the treatment-enriched, squamoid-basaloid and classical communities—displaying distinct malignant, stromal and immune cell-type compositions (Figure 4). The treatment-enriched community was preferably associated with the NEN, NRP, MES and ACN programs. Moreover, it was characterized by high infiltration of CD8⁺ T cells and neurotropic (NRT; neurogenesis and neuron differentiation pathway enrichment) and immunomodulatory (IMM; cytokine secretion and inflammation pathway upregulation) CAF signatures, reminiscent of the inflammatory CAF (iCAF) subtype initially identified in PDAC mouse models (see the section ‘CAF subtypes and function’). Conversely, the classical community, associated with the classical malignant program, showed exclusion of T cells and was characterized by infiltration of myeloid cells, specifically macrophages, neutrophils and conventional type 2 dendritic cells. This community also showed a high stroma content and upregulation of the myofibroblastic progenitor (MYO; high ACTA2 expression) and adhesive (ADH-F; enriched in cell-cell adhesion genes) CAF programs. Lastly, the squamoid-basaloid community, associated with the squamoid and basaloid malignant programs, displays a TME phenotype with higher and more diverse immune infiltration encompassing T_{regs}, B cells and myeloid cells, as well as lower stroma content compared with the classical community³⁹. This novel community classification shows how distinct PDAC subtypes shape their TME and how treatment modulates this composition. Functional studies are needed to elucidate the instructing mechanisms and to uncover associated therapeutic vulnerabilities.

Additional studies that integrated scRNA-seq or snRNA-seq and spatial transcriptomics datasets from human PDAC samples confirmed the previously reported enormous heterogeneity and the coexistence of tumor cells with distinct expression signatures^{41,57}. The analysis of 83 scRNA-seq or snRNA-seq samples and 15 spatial transcriptomics samples from 31 patients (ten treatment-naïve and 21 chemotherapy treated) revealed cancer cell subpopulations characterized by proliferation, KRAS signaling, cell stress and epithelial-to-mesenchymal (EMT) gene expression signatures⁵⁷. Multimodal intersection analysis was used for integration of scRNA-seq and spatial transcriptomics datasets, resulting in a cell-type tissue region map that elucidates the spatial distribution of cell types. PDAC cells showing high abundance of a stress response gene expression signature colocalized with the iCAF subtype— a main source of the cytokine interleukin 6 (IL-6), which is linked to the identified stress response signature in cancer cells⁴¹. Furthermore, and in accordance with the above-described data, treated PDAC specimens displaying chemoresistance exhibited a threefold enrichment of inflammatory CAFs, indicating that changes in the TME, as well as the stress response signature of the tumor cells, contribute at least in part to therapy resistance⁵⁷.

Single-cell profiling studies also shed light on the cells of origin of PDAC and its preneoplastic lesions, thereby providing clues on mechanisms underlying PDAC initiation^{57–60}. scRNA-seq based mapping of genetic changes to cell populations of patient samples uncovered transition stages of tumor development from normal cells to malignancy, such as acinar-to-ductal metaplasia, confirming data from genetically engineered mouse

models (GEMMs) of PDAC^{57,61}. These preclinical models recapitulate main aspects of human PDAC and are an invaluable toolkit for mechanistic studies. Accordingly, PDAC GEMMs have recently been extensively employed to functionalize and validate insights gained by single-cell profiling and to test therapeutic strategies, and we will discuss selected studies in the next paragraphs.

Acinar-to-ductal metaplasia is induced by tissue damage, such as acute and chronic pancreatitis, which promote KRAS-driven PDAC formation, but the underlying mechanisms remained largely unclear⁶⁰. Multimodal genomic analysis, including scATAC-seq profiling in PDAC GEMMs, revealed that tissue damage in combination with activation of oncogenic KRAS induces a cancer-associated epigenetic chromatin state in pancreatic acinar cells, which promotes cancer initiation⁶⁰. Mechanistically, tissue injury activates the cytokine IL-33 in epithelial cells, which cooperates with oncogenic KRAS to induce an acinar-to-neoplasia chromatin switch, thereby driving gene-regulatory programs that mediate neoplastic transformation⁶⁰. Single-cell analysis of tumor initiation in GEMMs of KRAS-driven PDAC revealed six distinct metaplastic cell types and states that originated from acinar cells⁵⁹. Although the contribution of the different metaplastic cell clusters to PDAC formation remains unclear, these data indicate that heterogeneity might occur at the earliest stages of PDAC formation⁵⁹. Interestingly, acinar metaplastic cells seem to instruct an immunosuppressive TME as early as in the pancreatic intraepithelial neoplasia state, for example, via recruitment of suppressive myeloid cell types and induction of dysfunctional CD4 T cells⁵⁹.

Tumor cell-TME interactions do not only have an important role in immunosuppression, but also in PDAC subtype specification. scRNA-seq analysis revealed that basal-like PDAC cells secrete C-C motif chemokine ligand 2 (CCL2), which is induced via bromodomain-containing protein 4 (BRD4)-mediated cJUN/AP1 expression. This secreted protein mediates recruitment of TNF-expressing macrophages, which in turn manifest the aggressive basal-like cell state of PDAC cells, serving as a mechanistic example of how cellular plasticity can be shaped by the TME⁶². To target the highly therapy-resistant mesenchymal PDAC subtype more efficiently, a novel combinatorial therapy consisting of the MEK inhibitor trametinib and the multikinase inhibitor nintedanib has been identified by high-throughput drug screening. This combination showed high selectivity for the mesenchymal subtype of the disease. Subsequent in vivo treatment studies and the integration of scRNA-seq analyses with secretomics revealed reprogramming of the immunosuppressive TME by a therapy-induced change of the cancer cell-derived secretome, resulting in infiltration of CD8⁺ T cells, thereby sensitizing the tumors to anti-programmed death-ligand 1 (PD-L1) immune checkpoint blockade (ICB)⁶³. These data show how the integration of scRNA-seq with other omics technologies can be used to infer therapy-induced changes in cell-cell communication or function and gain mechanistic insights into therapy response and resistance.

Subtype specification of PDAC substantially impacts TME diversity and the individual cell subsets and polarization states need to be investigated systematically to identify their biological function, as well as their therapeutic relevance. In the following section, we

will discuss recent single-cell approaches to deciphering the heterogeneity and function of individual cell subpopulations of the PDAC TME and their organization.

Composition and organization of the PDAC TME

Single-cell profiling has significantly contributed to the identification of distinct stromal and immune cell subpopulations and their phenotypic diversity. It not only enabled deconvolution of the context-dependent architecture and heterogeneity of the PDAC TME, as outlined above, but also provided first insights into the interaction, communication, organization and function of its various cell populations^{39,53,57,63}. The first scRNA-seq studies of human premalignant pancreatic lesions and PDAC, as well as GEMM PDAC models, revealed a striking cellular heterogeneity of the TME during tumor progression that converged into immunosuppression^{58,59,64–66}. In addition, approaches integrating scRNA-seq analysis with highly-multiplexed immunohistochemistry or spatial transcriptomics methods represent invaluable resources with which to investigate the phenotypic diversity and the cell-cell communication networks of individual TME cell types and associated niches in a spatial context^{39,41,57,67,68}. In the following paragraphs, we will focus on major cell types of the TME as discovered by single-cell profiling, as well as their functional relevance for the biology, phenotypic diversity and therapy of PDAC.

CAF subtypes and function

CAFs are attributed with a variety of functions, including ECM remodeling, crosstalk to immune and tumor cells, the secretion of growth and other soluble factors and regulating metabolic functions⁶⁹. Consequently, the role of CAFs is diverse and CAFs have been shown to exert context-dependent functions that can either be tumor promoting or tumor restraining by influencing tumor growth, immunosuppression and potentially tumor cell dissemination^{28,69–72}. While the origin of CAFs is controversial, experimental evidence suggests tissue-resident stellate cells (a cell population specific to the normal pancreas) as potential sources, which can be activated during tumorigenesis, leading to proliferation and formation of a dense fibroblast compartment²⁸.

CAF subtypes

In PDAC, two distinct CAF subpopulations have been identified first using immunofluorescence and RNA in situ hybridization⁷³. Myofibroblastic CAFs (myoCAFs) display high expression of α -smooth muscle actin (α SMA) and upregulation of TGF β signaling and are localized proximal to the tumor cells. In contrast, iCAFs are characterized by a secretory phenotype, high expression of IL-6 and leukemia inhibitory factor (LIF) and dispersed appearance within the tumor stroma^{73,74}. scRNA-seq of human and mouse PDAC tumors discovered a third CAF subpopulation termed antigen-presenting CAFs (apCAFs), which are characterized by high expression of major histocompatibility complex II and CD74, but lack the expression of costimulatory molecules⁷⁵.

Function of CAF subtypes and their specialized subsets

The advent of scRNA-seq enabled the fine mapping of the three major CAF subtypes and their specialized subsets⁶⁹, and provided first insights into their biology, as well as their functional role in promoting or restraining PDAC progression.

CAFs that secrete CXCL12 have been shown to block antitumor immunity via T cell exclusion⁷⁶, and CCL2 is implicated in the recruitment of immunosuppressive myeloid cells⁷⁷. Accordingly, Fap⁺ CAFs that are characterized by the upregulation of CXCL12 and CCL2 signaling are indeed tumor promoting and linked to significantly decreased overall survival of patients with PDAC^{78–80}. Genetic ablation of Fap⁺ CAFs in PDAC models resulted in a decrease of immunosuppressive myeloid cells and extended the survival time of the animals^{78–80}. Importantly, this CAF subpopulation displays opposing functions in PDAC progression as compared to α SMA⁺ myoCAFs, which are tumor-restraining and associated with increased overall survival of PDAC patients. Depletion of this CAF subtype increased immunosuppressive T_{reg} cells and decreased survival in mouse models^{71,78}. iCAFs have been shown to secrete IL-6 and LIF in PDAC⁷³, which drive immunosuppression by inducing the differentiation of suppressive MDSCs and the recruitment of TAMs, respectively^{57,77,81}. apCAFs have the capacity to present antigens to CD4⁺ T cells, but lack costimulatory molecules⁷⁵. Thus, T cell activation and proliferation cannot be induced. Instead, apCAFs ligate and induce T_{reg} cell differentiation and proliferation from naïve CD4⁺ T cells in vivo and thus block anti-tumor immunity⁸². These data demonstrate that several CAF subsets mediate immunosuppression. Identifying new ways to specifically target and reprogram these populations is an important area of research and holds the promise of unleashing antitumor immune responses.

Two non-interconvertible fibroblast lineages in the pancreas that can be distinguished by expression of the marker gene *CD105* have been recently identified. CD105⁺ CAFs display a tumor promoting phenotype, are more responsive to TGF β and show a higher abundance in PDAC, while CD105⁻ CAFs are tumor restrictive. Surprisingly, the CD105⁻ cells express mostly apCAF markers (major histocompatibility complex II (MHCII) and CD74), despite their tumor suppressive functions⁸³. Thus, specialized apCAF subtypes with opposing functions might exist, or their function might depend on the cellular and molecular context of the tumor, such as the molecular PDAC subtype and presence or absence of specific TME cell populations, such as CD4⁺ T cells and T_{reg} cells). These findings add another layer of complexity and further mechanistic studies are needed to elucidate the functional role of these two specific CAF subsets in context. A similar finding has been reported for the myoCAF subtype⁸⁴. scRNA-seq analysis of normal pancreas fibroblasts and CAFs revealed that a specific subset of myoCAFs, the TGF β -driven LRRC15⁺ myoCAF lineage, which constitutes the most abundant myoCAF subset in late-stage PDAC in GEMMs and human patients, correlated with poor responses to ICB in clinical trials⁸⁴. This suggests that LRRC15⁺ myoCAFs are another specialized CAF subpopulation that might exhibit immunosuppressive functions.

As described above, the advent of snRNA-seq enabled the in-depth single-cell multiomics and spatial characterization of human PDAC^{39,52,57}, including CAF subsets and their

transcriptional programs and states^{39,57}. Based on their expression profile, CAFs were defined as ADH-F, IMM, MYO and NRT³⁹. The MYO program is characterized by high expression of *ACTA2* and overlaps with the previously identified myoCAF expression signature. In addition, it shows upregulation of embryonic mesodermal development and Wnt pathway genes. The ADH-F, IMM and NRT CAF programs overlap with the previously described iCAF subtype and potentially represent different iCAF subsets, whereas apCAFs were not identified in this study. Upon therapy, the CAF compartment showed enrichment of the iCAF related ADH-F and IMM CAF transcriptional programs compared with untreated samples, indicating treatment-induced remodeling of the stroma and induction of iCAF subsets^{39,75}. In line with this, a strong enrichment of iCAFs has been linked to chemoresistance in human PDAC, indicating that this subtype or specialized subsets thereof might be promising targets to reprogram the tumor stroma to overcome therapy resistance⁵⁷.

The identification of distinct spatially confined subTMEs, which display deserted and reactive phenotypes linked to profound differences in the CAF and immune compartment, adds a spatial component to PDAC subtypes that has therapeutic and prognostic relevance⁸⁵. Reactive subTMEs displayed an immune hot phenotype and antitumor immune properties, whereas the ECM-rich deserted regions had fewer activated CAFs, were enriched upon chemotherapy and displayed chemoprotective features. Cultured CAFs originating from reactive subTMEs were enriched in EMT and TGF β signatures, as well as inflammatory gene sets, whereas cells derived from deserted subTMEs displayed growth-related gene sets (in line with a higher proliferation rate of these cultures) and lower expression of CAF activation markers⁸⁵. These results indicate again that CAF subpopulations are associated with specific PDAC phenotypes; however, further insights into the origin, marker gene expression and exact function of the specialized CAF subpopulations that might drive PDAC subTME specification are needed to integrate these findings into the framework of CAF-subtype function in PDAC.

scRNA-seq analyses are powerful tools to dissect novel therapeutic approaches and better understand their consequences, for example, in the context of targeting the desmoplastic PDAC stroma. Previous attempts to pharmacologically inhibit paracrine Hedgehog signaling- a pathway activated in CAFs that signals to PDAC cells and thereby dictates their growth and self renewal⁸⁶⁻⁸⁹-failed in clinical trials^{90,91}. Using scRNA-seq, Hedgehog pathway activity in distinct CAF subpopulations was interrogated, revealing that myoCAFs exhibit higher Hedgehog activity compared to iCAFs in mouse and human PDAC. Upon Hedgehog inhibition, the composition of the CAF compartment was altered and led to a decrease in myoCAFs but an increase in the iCAF subset and thereby a higher immunosuppressive activity⁹². This exemplifies the need to assess therapeutic responses of tumor cells and their TME holistically and to consider the phenotypic diversity and plasticity of cell types of the TME in PDAC subtypes.

CAF–cancer cell interactions

scRNA-seq of a human PDAC:CAF co-culture system revealed the existence of a proliferative (enriched in E2F target pathway signature) and EMT transcriptional PDAC cell program that is driven by CAFs⁹³. Interestingly, high CAF-to-PDAC ratios (ratio 90:10)

induced the co-expression of proliferative and EMT genes within individual PDAC cells (double-positive phenotype), whereas pure PDAC cell cultures were mainly double-negative phenotype, indicating that CAF-derived factors drive these transcriptional programs. Indeed, secretomic profiling of CAF conditioned medium identified TGF β -1 as a secreted factor inducing the transcriptional double-positive phenotype⁹³. However, the CAF subtype(s) that drive this process remain unclear and more studies are needed to dissect their complex cell-cell communication network.

Together, single-cell profiling revealed deep insights into CAF heterogeneity in human and mouse PDAC, and showed the existence of three distinct CAF subtypes as well as several specialized subpopulations, which exhibit opposing and context-specific functions. The underlying mechanisms that drive CAF heterogeneity and the exact context-dependent role of the diverse subpopulations remain widely enigmatic. Thus, there is a clear unmet need to map the full spectrum of specialized CAF subpopulations, assess their mechanistic role in context and probe their value as targets for therapeutic interventions. This will aid the development of novel therapeutic targeting approaches in the clinic (which were largely unsuccessful in the past) by focusing on vulnerabilities of specific CAF subpopulations and their context-dependent function^{69,88}. The systematic hierarchical classification of CAFs into broader populations and subpopulations with specialized functions, as proposed recently, will be an important step forward in the functional annotation of CAF subsets⁶⁹.

Other stromal cell types, such as pericytes, endothelial cells and nerves, are so far underrepresented in PDAC scRNA-seq studies, but are important to be considered in future analyses. Indeed, endothelial cell activation and increased endothelial expression of vascular cell adhesion protein 1 (VCAM1) through senescence-associated secretory phenotype induction in PDAC cells led to higher infiltration of CD8⁺ T cells and a more favorable ICB response in combination with a targeted combination therapy⁹⁴.

The immune landscape of PDAC

The PDAC immune TME is considered mainly immunosuppressive and often displays signs of T cell dysfunction or exclusion^{8,9,13}. CD8 T cells, if present, often lack markers of activation and display an exhausted phenotype, expressing, for example, high levels of PD-1, TIGIT, EOMES and GZMK^{8,9,11,68}. Besides, immunosuppressive myeloid cells infiltrate the PDAC TME at high levels^{95,96}. Accordingly, immunotherapies, such as ICB or engineered T cells failed in clinical trials in patients with PDAC^{13,97}. Only a small group of <1% of patients harboring microsatellite-unstable (MSI) hypermutated or *BRCA1*- and *BRCA2*-mutated homologous recombination-deficient PDACs with higher tumor mutational burden have benefited so far from ICB^{98–100}. However, response rates of MSI-high tumors are substantially lower than those of almost any other MSI-high cancer type¹⁰¹. Therefore, PDAC is considered one of the most immunotherapy-resistant tumors. This indicates, that a better understanding of the drivers of immunosuppression and T cell dysfunction that restrict immunotherapy response is urgently needed.

scRNA-seq unveiled unprecedented insights into the diversity and function of the PDAC immune landscape^{39,57,68,102,103}. Integration of scRNA-seq and CyTOF analyses of

treatment-naïve patients with PDAC and nonmalignant pancreas samples, established the first single-cell atlas that delineates the immune landscape of PDAC at large-scale⁶⁸. Importantly, fine-needle biopsy samples of patients with nonresectable advanced-stage PDAC-underrepresented in previous bulk-sequencing studies of mainly surgically resected tumors-were analyzed. These advanced tumors showed the highest level of T cell exhaustion, indicating ongoing T cell dysfunction. Generally, expression of immune checkpoints varied across immune cells as well as patients, indicating the need to further stratify these tumors and to identify the mechanisms that drive the observed heterogeneity of the PDAC immune landscape. Expression of the immune checkpoint TIGIT, which has been shown to regulate T cell- and natural killer cell-mediated cancer recognition and is typically found at high levels on T and natural killer cells, was correlated with T cell exhaustion, indicating a new possibility for TIGIT-directed immunotherapies^{57,68,104}. In line, the CD155/TIGIT ligand-immune receptor axis has been shown to mediate immune evasion in PDAC models, and targeting the axis in combination with PD-1 coinhibition and CD40 agonism induced anti-tumor immunity in vivo¹⁰⁴. Because TIGIT expression in PDAC is positively correlated with its occurrence in the patient's blood, it might represent a potential therapeutic biomarker of success of ICB or other immunotherapies⁶⁸.

T cells

The T cell landscape was further profiled by scRNA-seq of T cells and their T cell receptor (TCR-seq) in a cohort of 57 human PDAC patients¹⁰³. Thereby, distinct functional states of tumor-infiltrating lymphocytes (TILs) were characterized. Major CD8⁺ T cell subpopulations were annotated as CD8-GZMK (predysfunctional state), CD8-CXCL13 (exhausted state) and CD8-ZNF683 (tissue-resident memory state) TILs¹⁰³. The CD8-GZMK predysfunctional T cell population is defined by an intermediate clonality and low/intermediate expression of immune checkpoints and high expression of *GZMK* and *EOMES*. T cell receptor profiling and cell-state trajectory analysis revealed an overlap with cytotoxic (CD8-GZMB/PRF1) and exhausted/dysfunctional (CD8-CXCL13) CD8⁺ T cell populations, suggesting that CD8-GZMK cells represent an intermediate state between these populations that give rise to dysfunctional T cells¹⁰³. The CD8-CXCL13 T cell subset is characterized by high expression of the chemokine *CXCL13* and multiple immune checkpoints (for example, *CTLA4*, *PD1*, *TIM3*, *LAG3* and *TIGIT*) known to be present in dysfunctional and exhausted CD8⁺ T cells¹⁰³. The cytotoxic CD8⁺ state (CD8-GZMB/PRF1) is enriched in normal pancreas compared with PDAC and defined by expression of the effector T cell markers *GZMB*, *PRF1* and *TBX21*. The CD8-ZNF683 state is a putative tissue-resident memory CD8⁺ T cell state with potentially increased cytotoxic activity and reported to correlate with improved survival in other cancer entities. It is characterized by high expression of *ZNF683*, as well as tissue-resident memory CD8⁺ T cell-associated genes (for example, *XCL1* and *GNLY*), and low expression of *KLF2*¹⁰³. This scRNA-seq analysis serves as reference atlas for functional T cell subpopulations and needs to be expanded to TIL states in treated patients with PDAC to characterize TIL trajectories upon therapy.

The myeloid compartment

Integrating human and mouse PDAC scRNA-seq datasets provided novel insights into the myeloid cell compartment, specifically monocytes and macrophages¹⁰⁵. TAMs are characterized by high expression of the complement factors *CIQA*, *CIQB* and *TREM2*, which have an important role in regulating myeloid-mediated T cell exhaustion¹⁰⁶. Expression of *CIQ* complement factors induce the production of cytokines, as well as inflammatory responses¹⁰⁷. In addition, expression of *CIQA/B* has been observed in the blood of patients with PDAC, which could be used as potential prognostic biomarker to identify patients with high macrophage infiltration¹⁰⁸. Increased expression of *Trem2* in Arg1⁺ TAMs and monocytes has previously been linked to an immunosuppressive phenotype, and ablation of *Trem2* in mice led to a decrease in exhausted T cells and an increase in cytotoxic T and natural killer cells, indicating that these cells might be one of the main executors of immunosuppression¹⁰⁹. TAMs were further characterized by high expression of apolipoprotein E (APOE) in mouse and human PDAC. APOE has been shown to drive immunosuppression via nuclear factor κ B (NF- κ B) signaling by regulating *Cxcl1* expression in tumor cells and macrophages, which thereby recruit immunosuppressive MDSCs and suppress CD8⁺ T cell infiltration¹¹⁰. In addition, APOE serum levels in patient with PDAC correlated with a poor outcome, indicating prognostic relevance¹¹⁰.

Immunosuppressive immune signaling and cell-cell communication

scRNA-seq has also been used to infer cell-cell interaction networks and immune cell signaling hubs¹⁰², and these approaches can also be applied to in situ datasets generated by spatial profiling techniques, such as multiplexed immunohistochemistry or spatial transcriptomics, to characterize the architecture and spatial organization of the cancer cell-immune niche. Inference of ligand-receptor interaction pairs from scRNA-seq data has been employed to delineate cell-cell communication routes between malignant and TME cell types, such as the crosstalk between cell types, which mediate immunosuppression in primary and metastatic PDAC¹⁰². Epithelial cells showed the strongest connections with myeloid cells and potential immunosuppressive interactions with T cells, including the above-described and experimentally validated immune checkpoints PVR-TIGIT and PD1-PDCD1 (ligand expression on malignant cells)^{57,68,102,104}. These data demonstrate the power of single-cell analyses and computational methods to improve not only our understanding of immune cell composition in PDAC, but also potential immune function and mechanisms of immunosuppression. However, as stated above, functional studies are needed to validate candidate mechanisms and cell types mediating such immunosuppressive phenotypes.

Outlook and future challenges

The application of scRNA-seq in PDAC has led to a multitude of biological insights into heterogeneity, plasticity and response to therapy. One future challenge will be to set these findings into context and interrogate dependencies and cell-cell communication networks in a subtype-specific manner, or even map novel subtypes and dependencies from a cross-patient integrated single-cell PDAC atlas. This will enable the functionalization

of individual cell types and reveal their potential as therapeutic targets. Integrating scRNA-seq analyses and linking findings to the localization in the tumor by performing spatial transcriptomics approaches or histocytometry techniques will lead to important additional insights into the spatial organization of PDAC^{39,41,57,111}. Longitudinal single-cell analyses of tumorigenesis and treatment regimens will shed light on treatment-mediated effects on PDAC cells, their TME, their plasticity and resistance mechanisms. Future challenges include the identification and testing of effective subtype-specific therapies that target both the tumor cells and their protumorigenic environment. Genetic dependencies and potential therapeutic vulnerabilities can be inferred by conducting drug perturbation or CRISPR screens with scRNA-seq or spatial read-outs¹¹². Systematic large-scale screens, testing thousands of genes and hundreds of therapies in parallel¹¹³, can be integrated with machine learning to interrogate an interpolated perturbation space for designing optimal follow-up experiments¹¹⁴. These approaches offer the potential to rapidly advance our understanding of genetic and drug dependencies, and to identify new ways to target PDAC.

Acknowledgments

This study was supported by the German Cancer Consortium (DKTK), Deutsche Forschungsgemeinschaft (DFG SA 1374/8-1, Project-ID 515991405 to D.S.; DFG SA 1374/7-1, Project-ID 515571394 to D.S.; DGF SCHO 1732/2-1, Project-ID 360394750 to D.S.; DFG SA 1374/6-1, Project ID 458890590 to D.S.; DFG SA 1374/4-3, Project ID 219542602 to D.S.; SFB 1321 Project-ID 329628492 P06, P11 and S01 to R.R. and D.S.), the Wilhelm Sander-Stiftung (2020.174.1 and 2017.091.2 to D.S.), and the European Research Council (ERC CoG No. 648521 to D.S.). C.F. is a Cancer Research Institute Irvington Fellow supported by the Cancer Research Institute (CRI4641).

References

1. Siegel RL, Miller KD, Wagle NS, Jemal A. Cancer statistics, 2023. *CA Cancer J Clin.* 2023; 73: 17–48. DOI: 10.3322/caac.21763 [PubMed: 36633525]
2. Rahib L, Wehner MR, Matrisian LM, Nead KT. Estimated Projection of US Cancer Incidence and Death to 2040. *JAMA Netw Open.* 2021; 4 e214708 doi: 10.1001/jamanetworkopen.2021.4708 [PubMed: 33825840]
3. Waddell N, et al. Whole genomes redefine the mutational landscape of pancreatic cancer. *Nature.* 2015; 518: 495–501. DOI: 10.1038/nature14169 [PubMed: 25719666]
4. Witkiewicz AK, et al. Whole-exome sequencing of pancreatic cancer defines genetic diversity and therapeutic targets. *Nat Commun.* 2015; 6 6744 doi: 10.1038/ncomms7744 [PubMed: 25855536]
5. Connor AA, Gallinger S. Pancreatic cancer evolution and heterogeneity: integrating omics and clinical data. *Nat Rev Cancer.* 2022; 22: 131–142. DOI: 10.1038/s41568-021-00418-1 [PubMed: 34789870]
6. Aung KL, et al. Genomics-Driven Precision Medicine for Advanced Pancreatic Cancer: Early Results from the COMPASS Trial. *Clin Cancer Res.* 2018; 24: 1344–1354. DOI: 10.1158/1078-0432.Ccr-17-2994 [PubMed: 29288237]
7. Chan-Seng-Yue M, et al. Transcription phenotypes of pancreatic cancer are driven by genomic events during tumor evolution. *Nat Genet.* 2020; 52: 231–240. DOI: 10.1038/s41588-019-0566-9 [PubMed: 31932696]
8. Falcomatà C, et al. Context-Specific Determinants of the Immunosuppressive Tumor Microenvironment in Pancreatic Cancer. *Cancer Discov.* 2023; Of1–of20. DOI: 10.1158/2159-8290.Cd-22-0876
9. Binnewies M, et al. Understanding the tumor immune microenvironment (TIME) for effective therapy. *Nat Med.* 2018; 24: 541–550. DOI: 10.1038/s41591-018-0014-x [PubMed: 29686425]

10. Carstens JL, et al. Spatial computation of intratumoral T cells correlates with survival of patients with pancreatic cancer. *Nat Commun.* 2017; 8 15095 doi: 10.1038/ncomms15095 [PubMed: 28447602]
11. Liudahl SM, et al. Leukocyte Heterogeneity in Pancreatic Ductal Adenocarcinoma: Phenotypic and Spatial Features Associated with Clinical Outcome. *Cancer Discov.* 2021; 11: 2014–2031. DOI: 10.1158/2159-8290.Cd-20-0841 [PubMed: 33727309]
12. Mahajan UM, et al. Immune Cell and Stromal Signature Associated With Progression-Free Survival of Patients With Resected Pancreatic Ductal Adenocarcinoma. *Gastroenterology.* 2018; 155: 1625–1639. e1622 doi: 10.1053/j.gastro.2018.08.009 [PubMed: 30092175]
13. Bear AS, Vonderheide RH, O’Hara MH. Challenges and Opportunities for Pancreatic Cancer Immunotherapy. *Cancer Cell.* 2020; 38: 788–802. DOI: 10.1016/j.ccell.2020.08.004 [PubMed: 32946773]
14. Hosein AN, Brekken RA, Maitra A. Pancreatic cancer stroma: an update on therapeutic targeting strategies. *Nat Rev Gastroenterol Hepatol.* 2020; 17: 487–505. DOI: 10.1038/s41575-020-0300-1 [PubMed: 32393771]
15. Neesse A, Algül H, Tuveson DA, Gress TM. Stromal biology and therapy in pancreatic cancer: a changing paradigm. *Gut.* 2015; 64: 1476–1484. DOI: 10.1136/gutjnl-2015-309304 [PubMed: 25994217]
16. Moffitt RA, et al. Virtual microdissection identifies distinct tumor- and stroma-specific subtypes of pancreatic ductal adenocarcinoma. *Nat Genet.* 2015; 47: 1168–1178. DOI: 10.1038/ng.3398 [PubMed: 26343385]
17. Mueller S, et al. Evolutionary routes and KRAS dosage define pancreatic cancer phenotypes. *Nature.* 2018; 554: 62–68. DOI: 10.1038/nature25459 [PubMed: 29364867]
18. Miyabayashi K, et al. Intraductal Transplantation Models of Human Pancreatic Ductal Adenocarcinoma Reveal Progressive Transition of Molecular Subtypes. *Cancer Discov.* 2020; 10: 1566–1589. DOI: 10.1158/2159-8290.Cd-20-0133 [PubMed: 32703770]
19. Bailey P, et al. Genomic analyses identify molecular subtypes of pancreatic cancer. *Nature.* 2016; 531: 47–52. DOI: 10.1038/nature16965 [PubMed: 26909576]
20. Collisson EA, Bailey P, Chang DK, Biankin AV. Molecular subtypes of pancreatic cancer. *Nat Rev Gastroenterol Hepatol.* 2019; 16: 207–220. DOI: 10.1038/s41575-019-0109-y [PubMed: 30718832]
21. Collisson EA, et al. Subtypes of pancreatic ductal adenocarcinoma and their differing responses to therapy. *Nat Med.* 2011; 17: 500–503. DOI: 10.1038/nm.2344 [PubMed: 21460848]
22. Dijk F, et al. Unsupervised class discovery in pancreatic ductal adenocarcinoma reveals cell-intrinsic mesenchymal features and high concordance between existing classification systems. *Sci Rep.* 2020; 10: 337. doi: 10.1038/s41598-019-56826-9 [PubMed: 31941932]
23. Kalimuthu N, et al. Morphological classification of pancreatic ductal adenocarcinoma that predicts molecular subtypes and correlates with clinical outcome. *Gut.* 2020; 69: 317–328. DOI: 10.1136/gutjnl-2019-318217 [PubMed: 31201285]
24. Le Large TY, et al. Microdissected pancreatic cancer proteomes reveal tumor heterogeneity and therapeutic targets. *JCI Insight.* 2020; 5 doi: 10.1172/jci.insight.138290
25. Milan M, Diaferia GR, Natoli G. Tumor cell heterogeneity and its transcriptional bases in pancreatic cancer: a tale of two cell types and their many variants. *Embo j.* 2021; 40 e107206 doi: 10.15252/embj.2020107206 [PubMed: 33844319]
26. Olive KP, et al. Inhibition of Hedgehog signaling enhances delivery of chemotherapy in a mouse model of pancreatic cancer. *Science (New York, NY).* 2009; 324: 1457–1461. DOI: 10.1126/science.1171362
27. Hayashi A, et al. A unifying paradigm for transcriptional heterogeneity and squamous features in pancreatic ductal adenocarcinoma. *Nat Cancer.* 2020; 1: 59–74. DOI: 10.1038/s43018-019-0010-1 [PubMed: 35118421]
28. Sahai E, et al. A framework for advancing our understanding of cancer-associated fibroblasts. *Nat Rev Cancer.* 2020; 20: 174–186. DOI: 10.1038/s41568-019-0238-1 [PubMed: 31980749]

29. Steins A, et al. High-grade mesenchymal pancreatic ductal adenocarcinoma drives stromal deactivation through CSF-1. *EMBO Rep.* 2020; 21 e48780 doi: 10.15252/embr.201948780 [PubMed: 32173982]
30. Puleo F, et al. Stratification of Pancreatic Ductal Adenocarcinomas Based on Tumor and Microenvironment Features. *Gastroenterology.* 2018; 155: 1999–2013. e1993 doi: 10.1053/j.gastro.2018.08.033 [PubMed: 30165049]
31. Giladi A, Amit I. Single-Cell Genomics: A Stepping Stone for Future Immunology Discoveries. *Cell.* 2018; 172: 14–21. DOI: 10.1016/j.cell.2017.11.011 [PubMed: 29328909]
32. Sun G, et al. Single-cell RNA sequencing in cancer: Applications, advances, and emerging challenges. *Mol Ther Oncolytics.* 2021; 21: 183–206. DOI: 10.1016/j.omto.2021.04.001 [PubMed: 34027052]
33. Yofe I, Dahan R, Amit I. Single-cell genomic approaches for developing the next generation of immunotherapies. *Nat Med.* 2020; 26: 171–177. DOI: 10.1038/s41591-019-0736-4 [PubMed: 32015555]
34. Casado-Pelaez M, Bueno-Costa A, Esteller M. Single cell cancer epigenetics. *Trends in Cancer.* doi: 10.1016/j.trecan.2022.06.005
35. Jia Q, Chu H, Jin Z, Long H, Zhu B. High-throughput single-cell sequencing in cancer research. *Signal Transduct Target Ther.* 2022; 7: 145. doi: 10.1038/s41392-022-00990-4 [PubMed: 35504878]
36. Method of the Year 2019: Single-cell multimodal omics. *Nat Methods.* 2020; 17: 1. doi: 10.1038/s41592-019-0703-5 [PubMed: 31907477]
37. Palla G, Fischer DS, Regev A, Theis FJ. Spatial components of molecular tissue biology. *Nat Biotechnol.* 2022; 40: 308–318. DOI: 10.1038/s41587-021-01182-1 [PubMed: 35132261]
38. Smith EA, Hodges HC. The Spatial and Genomic Hierarchy of Tumor Ecosystems Revealed by Single-Cell Technologies. *Trends Cancer.* 2019; 5: 411–425. DOI: 10.1016/j.trecan.2019.05.009 [PubMed: 31311656]
39. Hwang WL, et al. Single-nucleus and spatial transcriptome profiling of pancreatic cancer identifies multicellular dynamics associated with neoadjuvant treatment. *Nat Genet.* 2022; doi: 10.1038/s41588-022-01134-8
40. Merritt CR, et al. Multiplex digital spatial profiling of proteins and RNA in fixed tissue. *Nat Biotechnol.* 2020; 38: 586–599. DOI: 10.1038/s41587-020-0472-9 [PubMed: 32393914]
41. Moncada R, et al. Integrating microarray-based spatial transcriptomics and single-cell RNA-seq reveals tissue architecture in pancreatic ductal adenocarcinomas. *Nat Biotechnol.* 2020; 38: 333–342. DOI: 10.1038/s41587-019-0392-8 [PubMed: 31932730]
42. Colomé-Tatché M, Theis FJ. Statistical single cell multi-omics integration. *Current Opinion in Systems Biology.* 2018; 7: 54–59. DOI: 10.1016/j.coisb.2018.01.003
43. Hao Y, et al. Integrated analysis of multimodal single-cell data. *Cell.* 2021; 184: 3573–3587. e3529 doi: 10.1016/j.cell.2021.04.048 [PubMed: 34062119]
44. Kharchenko PV. The triumphs and limitations of computational methods for scRNA-seq. *Nat Methods.* 2021; 18: 723–732. DOI: 10.1038/s41592-021-01171-x [PubMed: 34155396]
45. Luecken MD, Theis FJ. Current best practices in single-cell RNA-seq analysis: a tutorial. *Mol Syst Biol.* 2019; 15 e8746 doi: 10.15252/msb.20188746 [PubMed: 31217225]
46. Argelaguet R, Cuomo ASE, Stegle O, Marioni JC. Computational principles and challenges in single-cell data integration. *Nat Biotechnol.* 2021; 39: 1202–1215. DOI: 10.1038/s41587-021-00895-7 [PubMed: 33941931]
47. Regev A, et al. The Human Cell Atlas. *eLife.* 2017; 6 e27041 doi: 10.7554/eLife.27041 [PubMed: 29206104]
48. Lotfollahi M, et al. Mapping single-cell data to reference atlases by transfer learning. *Nat Biotechnol.* 2022; 40: 121–130. DOI: 10.1038/s41587-021-01001-7 [PubMed: 34462589]
49. Cao ZJ, Gao G. Multi-omics single-cell data integration and regulatory inference with graph-linked embedding. *Nat Biotechnol.* 2022; 40: 1458–1466. DOI: 10.1038/s41587-022-01284-4 [PubMed: 35501393]
50. Hao Y, et al. Dictionary learning for integrative, multimodal, and scalable single-cell analysis. *bioRxiv.* 2022; 2022.2002.2024.481684 doi: 10.1101/2022.02.24.481684

51. Lotfollahi M, Litinetskaya A, Theis FJ. Multigrade: single-cell multi-omic data integration. *bioRxiv*. 2022; 2022.2003.2016.484643 doi: 10.1101/2022.03.16.484643
52. Han J, DePinho RA, Maitra A. Single-cell RNA sequencing in pancreatic cancer. *Nat Rev Gastroenterol Hepatol*. 2021; 18: 451–452. DOI: 10.1038/s41575-021-00471-z [PubMed: 34040169]
53. Raghavan S, et al. Microenvironment drives cell state, plasticity, and drug response in pancreatic cancer. *Cell*. 2021; 184: 6119–6137. e6126 doi: 10.1016/j.cell.2021.11.017 [PubMed: 34890551]
54. Ting DT, et al. Single-cell RNA sequencing identifies extracellular matrix gene expression by pancreatic circulating tumor cells. *Cell Rep*. 2014; 8: 1905–1918. DOI: 10.1016/j.celrep.2014.08.029 [PubMed: 25242334]
55. Krieger TG, et al. Single-cell analysis of patient-derived PDAC organoids reveals cell state heterogeneity and a conserved developmental hierarchy. *Nat Commun*. 2021; 12 5826 doi: 10.1038/s41467-021-26059-4 [PubMed: 34611171]
56. Chijimatsu R, et al. Establishment of a reference single-cell RNA sequencing dataset for human pancreatic adenocarcinoma. *iScience*. 2022; 25 104659 doi: 10.1016/j.isci.2022.104659 [PubMed: 35847558]
57. Cui Zhou D, et al. Spatially restricted drivers and transitional cell populations cooperate with the microenvironment in untreated and chemo-resistant pancreatic cancer. *Nat Genet*. 2022; 54: 1390–1405. DOI: 10.1038/s41588-022-01157-1 [PubMed: 35995947]
58. Bernard V, et al. Single-Cell Transcriptomics of Pancreatic Cancer Precursors Demonstrates Epithelial and Microenvironmental Heterogeneity as an Early Event in Neoplastic Progression. *Clin Cancer Res*. 2019; 25: 2194–2205. DOI: 10.1158/1078-0432.Ccr-18-1955 [PubMed: 30385653]
59. Schlesinger Y, et al. Single-cell transcriptomes of pancreatic preinvasive lesions and cancer reveal acinar metaplastic cells' heterogeneity. *Nat Commun*. 2020; 11 4516 doi: 10.1038/s41467-020-18207-z [PubMed: 32908137]
60. Alonso-Curbelo D, et al. A gene-environment-induced epigenetic program initiates tumorigenesis. *Nature*. 2021; 590: 642–648. DOI: 10.1038/s41586-020-03147-x [PubMed: 33536616]
61. Storz P. Acinar cell plasticity and development of pancreatic ductal adenocarcinoma. *Nat Rev Gastroenterol Hepatol*. 2017; 14: 296–304. DOI: 10.1038/nrgastro.2017.12 [PubMed: 28270694]
62. Tu M, et al. TNF- α -producing macrophages determine subtype identity and prognosis via API enhancer reprogramming in pancreatic cancer. *Nat Cancer*. 2021; 2: 1185–1203. DOI: 10.1038/s43018-021-00258-w [PubMed: 35122059]
63. Falcomatà C, et al. Selective multi-kinase inhibition sensitizes mesenchymal pancreatic cancer to immune checkpoint blockade by remodeling the tumor microenvironment. *Nat Cancer*. 2022; doi: 10.1038/s43018-021-00326-1
64. Hosein AN, et al. Cellular heterogeneity during mouse pancreatic ductal adenocarcinoma progression at single-cell resolution. *JCI Insight*. 2019; 5 doi: 10.1172/jci.insight.129212
65. Ischenko I, et al. KRAS drives immune evasion in a genetic model of pancreatic cancer. *Nat Commun*. 2021; 12 1482 doi: 10.1038/s41467-021-21736-w [PubMed: 33674596]
66. Peng J, et al. Single-cell RNA-seq highlights intra-tumoral heterogeneity and malignant progression in pancreatic ductal adenocarcinoma. *Cell Res*. 2019; 29: 725–738. DOI: 10.1038/s41422-019-0195-y [PubMed: 31273297]
67. Andersson A, et al. Spatial deconvolution of HER2-positive breast cancer delineates tumor-associated cell type interactions. *Nat Commun*. 2021; 12 6012 doi: 10.1038/s41467-021-26271-2 [PubMed: 34650042]
68. Steele NG, et al. Multimodal Mapping of the Tumor and Peripheral Blood Immune Landscape in Human Pancreatic Cancer. *Nat Cancer*. 2020; 1: 1097–1112. DOI: 10.1038/s43018-020-00121-4 [PubMed: 34296197]
69. Lavie D, Ben-Shmuel A, Erez N, Scherz-Shouval R. Cancer-associated fibroblasts in the single-cell era. *Nat Cancer*. 2022; 3: 793–807. DOI: 10.1038/s43018-022-00411-z [PubMed: 35883004]
70. Hwang RF, et al. Cancer-associated stromal fibroblasts promote pancreatic tumor progression. *Cancer Res*. 2008; 68: 918–926. DOI: 10.1158/0008-5472.Can-07-5714 [PubMed: 18245495]

71. Özdemir BC, et al. Depletion of carcinoma-associated fibroblasts and fibrosis induces immunosuppression and accelerates pancreas cancer with reduced survival. *Cancer Cell*. 2014; 25: 719–734. DOI: 10.1016/j.ccr.2014.04.005 [PubMed: 24856586]
72. Rhim AD, et al. Stromal elements act to restrain, rather than support, pancreatic ductal adenocarcinoma. *Cancer Cell*. 2014; 25: 735–747. DOI: 10.1016/j.ccr.2014.04.021 [PubMed: 24856585]
73. Öhlund D, et al. Distinct populations of inflammatory fibroblasts and myofibroblasts in pancreatic cancer. *J Exp Med*. 2017; 214: 579–596. DOI: 10.1084/jem.20162024 [PubMed: 28232471]
74. Biffi G, et al. IL1-Induced JAK/STAT Signaling Is Antagonized by TGF β to Shape CAF Heterogeneity in Pancreatic Ductal Adenocarcinoma. *Cancer Discov*. 2019; 9: 282–301. DOI: 10.1158/2159-8290.Cd-18-0710 [PubMed: 30366930]
75. Elyada E, et al. Cross-Species Single-Cell Analysis of Pancreatic Ductal Adenocarcinoma Reveals Antigen-Presenting Cancer-Associated Fibroblasts. *Cancer Discov*. 2019; 9: 1102–1123. DOI: 10.1158/2159-8290.Cd-19-0094 [PubMed: 31197017]
76. Feig C, et al. Targeting CXCL12 from FAP-expressing carcinoma-associated fibroblasts synergizes with anti-PD-L1 immunotherapy in pancreatic cancer. *Proc Natl Acad Sci U S A*. 2013; 110: 20212–20217. DOI: 10.1073/pnas.1320318110 [PubMed: 24277834]
77. Hallett R, et al. Therapeutic targeting of LIF overcomes macrophage mediated immunosuppression of the local tumor microenvironment. *Clinical Cancer Research*. 2022; doi: 10.1158/1078-0432.Ccr-21-1888
78. McAndrews KM, et al. Identification of Functional Heterogeneity of Carcinoma-Associated Fibroblasts with Distinct IL6-Mediated Therapy Resistance in Pancreatic Cancer. *Cancer Discov*. 2022; 12: 1580–1597. DOI: 10.1158/2159-8290.Cd-20-1484 [PubMed: 35348629]
79. Lo A, et al. Fibroblast activation protein augments progression and metastasis of pancreatic ductal adenocarcinoma. *JCI Insight*. 2017; 2 doi: 10.1172/jci.insight.92232
80. Yang X, et al. FAP Promotes Immunosuppression by Cancer-Associated Fibroblasts in the Tumor Microenvironment via STAT3-CCL2 Signaling. *Cancer Res*. 2016; 76: 4124–4135. DOI: 10.1158/0008-5472.Can-15-2973 [PubMed: 27216177]
81. Weber R, et al. IL-6 as a major regulator of MDSC activity and possible target for cancer immunotherapy. *Cellular Immunology*. 2021; 359 104254 doi: 10.1016/j.cellimm.2020.104254 [PubMed: 33296753]
82. Huang H, et al. Mesothelial cell-derived antigen-presenting cancer-associated fibroblasts induce expansion of regulatory T cells in pancreatic cancer. *Cancer Cell*. 2022; doi: 10.1016/j.ccell.2022.04.011
83. Hutton C, et al. Single-cell analysis defines a pancreatic fibroblast lineage that supports anti-tumor immunity. *Cancer Cell*. 2021; 39: 1227–1244. e1220 doi: 10.1016/j.ccell.2021.06.017 [PubMed: 34297917]
84. Dominguez CX, et al. Single-Cell RNA Sequencing Reveals Stromal Evolution into LRRC15(+) Myofibroblasts as a Determinant of Patient Response to Cancer Immunotherapy. *Cancer Discov*. 2020; 10: 232–253. DOI: 10.1158/2159-8290.Cd-19-0644 [PubMed: 31699795]
85. Grünwald BT, et al. Spatially confined sub-tumor microenvironments in pancreatic cancer. *Cell*. 2021; 184: 5577–5592. e5518 doi: 10.1016/j.cell.2021.09.022 [PubMed: 34644529]
86. Falcomatà C, Saur D. Self-renewal equality in pancreas homeostasis, regeneration, and cancer. *Cell Rep*. 2021; 37 110135 doi: 10.1016/j.celrep.2021.110135 [PubMed: 34910913]
87. Lee JJ, et al. Stromal response to Hedgehog signaling restrains pancreatic cancer progression. *Proc Natl Acad Sci U S A*. 2014; 111: E3091–3100. DOI: 10.1073/pnas.1411679111 [PubMed: 25024225]
88. Lodestijn SC, et al. Marker-free lineage tracing reveals an environment-instructed clonogenic hierarchy in pancreatic cancer. *Cell Rep*. 2021; 37 109852 doi: 10.1016/j.celrep.2021.109852 [PubMed: 34686335]
89. Scales MK, et al. Combinatorial Gli activity directs immune infiltration and tumor growth in pancreatic cancer. *PLoS Genet*. 2022; 18 e1010315 doi: 10.1371/journal.pgen.1010315 [PubMed: 35867772]

90. Catenacci DV, et al. Randomized Phase Ib/II Study of Gemcitabine Plus Placebo or Vismodegib, a Hedgehog Pathway Inhibitor, in Patients With Metastatic Pancreatic Cancer. *J Clin Oncol.* 2015; 33: 4284–4292. DOI: 10.1200/jco.2015.62.8719 [PubMed: 26527777]
91. Ko AH, et al. A Phase I Study of FOLFIRINOX Plus IPI-926, a Hedgehog Pathway Inhibitor, for Advanced Pancreatic Adenocarcinoma. *Pancreas.* 2016; 45: 370–375. DOI: 10.1097/mpa.0000000000000458 [PubMed: 26390428]
92. Steele NG, et al. Inhibition of Hedgehog Signaling Alters Fibroblast Composition in Pancreatic Cancer. *Clin Cancer Res.* 2021; 27: 2023–2037. DOI: 10.1158/1078-0432.Ccr-20-3715 [PubMed: 33495315]
93. Ligorio M, et al. Stromal Microenvironment Shapes the Intratumoral Architecture of Pancreatic Cancer. *Cell.* 2019; 178: 160–175. e127 doi: 10.1016/j.cell.2019.05.012 [PubMed: 31155233]
94. Ruscetti M, et al. Senescence-Induced Vascular Remodeling Creates Therapeutic Vulnerabilities in Pancreas Cancer. *Cell.* 2021; 184: 4838–4839. DOI: 10.1016/j.cell.2021.07.028 [PubMed: 34478658]
95. Veglia F, Sanseviero E, Gabrilovich DI. Myeloid-derived suppressor cells in the era of increasing myeloid cell diversity. *Nat Rev Immunol.* 2021; 21: 485–498. DOI: 10.1038/s41577-020-00490-y [PubMed: 33526920]
96. Zhu Y, et al. Tissue-Resident Macrophages in Pancreatic Ductal Adenocarcinoma Originate from Embryonic Hematopoiesis and Promote Tumor Progression. *Immunity.* 2017; 47: 323–338. e326 doi: 10.1016/j.immuni.2017.07.014 [PubMed: 28813661]
97. Renouf DJ, et al. The CCTG PA.7 phase II trial of gemcitabine and nab-paclitaxel with or without durvalumab and tremelimumab as initial therapy in metastatic pancreatic ductal adenocarcinoma. *Nat Commun.* 2022; 13 5020 doi: 10.1038/s41467-022-32591-8 [PubMed: 36028483]
98. Terrero G, et al. Ipilimumab/Nivolumab Therapy in Patients With Metastatic Pancreatic or Biliary Cancer With Homologous Recombination Deficiency Pathogenic Germline Variants. *JAMA Oncol.* 2022; 8: 1–3. DOI: 10.1001/jamaoncol.2022.0611
99. Luchini C, et al. Comprehensive characterisation of pancreatic ductal adenocarcinoma with microsatellite instability: histology, molecular pathology and clinical implications. *Gut.* 2021; 70: 148–156. DOI: 10.1136/gutjnl-2020-320726 [PubMed: 32350089]
100. Reiss KA, et al. Niraparib plus nivolumab or niraparib plus ipilimumab in patients with platinum-sensitive advanced pancreatic cancer: a randomised, phase 1b/2 trial. *Lancet Oncol.* 2022; 23: 1009–1020. DOI: 10.1016/s1470-2045(22)00369-2 [PubMed: 35810751]
101. Marabelle A, et al. Efficacy of Pembrolizumab in Patients With Noncolorectal High Microsatellite Instability/Mismatch Repair-Deficient Cancer: Results From the Phase II KEYNOTE-158 Study. *J Clin Oncol.* 2020; 38: 1–10. DOI: 10.1200/jco.19.02105 [PubMed: 31682550]
102. Lee JJ, et al. Elucidation of Tumor-Stromal Heterogeneity and the Ligand-Receptor Interactome by Single-Cell Transcriptomics in Real-world Pancreatic Cancer Biopsies. *Clin Cancer Res.* 2021; 27: 5912–5921. DOI: 10.1158/1078-0432.Ccr-20-3925 [PubMed: 34426439]
103. Schalck A, et al. Single cell sequencing reveals trajectory of tumor-infiltrating lymphocyte states in pancreatic cancer. *Cancer Discov.* 2022; doi: 10.1158/2159-8290.Cd-21-1248
104. Freed-Pastor WA, et al. The CD155/TIGIT axis promotes and maintains immune evasion in neoantigen-expressing pancreatic cancer. *Cancer Cell.* 2021; 39: 1342–1360. e1314 doi: 10.1016/j.ccell.2021.07.007 [PubMed: 34358448]
105. Kadiyala P, Elhossiny AM, Carpenter ES. Using Single Cell Transcriptomics to Elucidate the Myeloid Compartment in Pancreatic Cancer. *Front Oncol.* 2022; 12 881871 doi: 10.3389/fonc.2022.881871 [PubMed: 35664793]
106. Binnewies M, et al. Targeting TREM2 on tumor-associated macrophages enhances immunotherapy. *Cell Rep.* 2021; 37 109844 doi: 10.1016/j.celrep.2021.109844 [PubMed: 34686340]
107. Bohlsón SS, O’Conner SD, Hulsebus HJ, Ho MM, Fraser DA. Complement, c1q, and c1q-related molecules regulate macrophage polarization. *Front Immunol.* 2014; 5: 402. doi: 10.3389/fimmu.2014.00402 [PubMed: 25191325]
108. Kemp SB, et al. Pancreatic cancer is marked by complement-high blood monocytes and tumor-associated macrophages. *Life Sci Alliance.* 2021; 4 doi: 10.26508/lsa.202000935

109. Katzenelenbogen Y, et al. Coupled scRNA-Seq and Intracellular Protein Activity Reveal an Immunosuppressive Role of TREM2 in Cancer. *Cell*. 2020; 182: 872–885. e819 doi: 10.1016/j.cell.2020.06.032 [PubMed: 32783915]
110. Kemp SB, et al. Apolipoprotein E Promotes Immune Suppression in Pancreatic Cancer through NF- κ B-Mediated Production of CXCL1. *Cancer Res*. 2021; 81: 4305–4318. DOI: 10.1158/0008-5472.Can-20-3929 [PubMed: 34049975]
111. Longo SK, Guo MG, Ji AL, Khavari PA. Integrating single-cell and spatial transcriptomics to elucidate intercellular tissue dynamics. *Nat Rev Genet*. 2021; 22: 627–644. DOI: 10.1038/s41576-021-00370-8 [PubMed: 34145435]
112. Dhainaut M, et al. Spatial CRISPR genomics identifies regulators of the tumor microenvironment. *Cell*. 2022; 185: 1223–1239. e1220 doi: 10.1016/j.cell.2022.02.015 [PubMed: 35290801]
113. Dixit A, et al. Perturb-Seq: Dissecting Molecular Circuits with Scalable Single-Cell RNA Profiling of Pooled Genetic Screens. *Cell*. 2016; 167: 1853–1866. e1817 doi: 10.1016/j.cell.2016.11.038 [PubMed: 27984732]
114. Ji Y, Lotfollahi M, Wolf FA, Theis FJ. Machine learning for perturbational single-cell omics. *Cell Syst*. 2021; 12: 522–537. DOI: 10.1016/j.cels.2021.05.016 [PubMed: 34139164]
115. Juiz N, et al. Basal-like and classical cells coexist in pancreatic cancer revealed by single-cell analysis on biopsy-derived pancreatic cancer organoids from the classical subtype. *Faseb j*. 2020; 34: 12214–12228. DOI: 10.1096/fj.202000363RR [PubMed: 32686876]
116. Lin W, et al. Single-cell transcriptome analysis of tumor and stromal compartments of pancreatic ductal adenocarcinoma primary tumors and metastatic lesions. *Genome Med*. 2020; 12: 80. doi: 10.1186/s13073-020-00776-9 [PubMed: 32988401]
117. Tosti L, et al. Single-Nucleus and In Situ RNA-Sequencing Reveal Cell Topographies in the Human Pancreas. *Gastroenterology*. 2021; 160: 1330–1344. e1311 doi: 10.1053/j.gastro.2020.11.010 [PubMed: 33212097]
118. Stoeckius M, et al. Simultaneous epitope and transcriptome measurement in single cells. *Nat Methods*. 2017; 14: 865–868. DOI: 10.1038/nmeth.4380 [PubMed: 28759029]
119. Mimitou EP, et al. Scalable, multimodal profiling of chromatin accessibility, gene expression and protein levels in single cells. *Nat Biotechnol*. 2021; 39: 1246–1258. DOI: 10.1038/s41587-021-00927-2 [PubMed: 34083792]
120. Armingol E, Officer A, Harismendy O, Lewis NE. Deciphering cell-cell interactions and communication from gene expression. *Nat Rev Genet*. 2021; 22: 71–88. DOI: 10.1038/s41576-020-00292-x [PubMed: 33168968]
121. Fischer DS, Schaar AC, Theis FJ. Modeling intercellular communication in tissues using spatial graphs of cells. *Nat Biotechnol*. 2022; doi: 10.1038/s41587-022-01467-z
122. Giladi A, et al. Dissecting cellular crosstalk by sequencing physically interacting cells. *Nat Biotechnol*. 2020; 38: 629–637. DOI: 10.1038/s41587-020-0442-2 [PubMed: 32152598]
123. Marx V. Method of the Year: spatially resolved transcriptomics. *Nat Methods*. 2021; 18: 9–14. DOI: 10.1038/s41592-020-01033-y [PubMed: 33408395]
124. Zhao E, et al. Spatial transcriptomics at subspot resolution with BayesSpace. *Nat Biotechnol*. 2021; 39: 1375–1384. DOI: 10.1038/s41587-021-00935-2 [PubMed: 34083791]

Box 1**Advanced single-cell and spatial profiling technologies and tools**

scRNA-seq and spatial profiling technologies are rapidly evolving^{31–35,37,38,42–46} (Figure 1-3). The combination of scRNA-seq or spatial transcriptomics with DNA-barcoded antibodies allows simultaneous surface protein profiling (cellular indexing of transcriptomics and epitopes by sequencing (CITE-seq)) to enhance phenotyping by using cell-type and functional markers¹¹⁸ (Figure 2). This method was further complemented to assess proteomic features, as well as the chromatin state of the respective cells, by combination with sparse scATAC-seq (ASAP-seq)¹¹⁹. In addition, scRNA-seq can be utilized to investigate cell-cell communication by assessing the gene expression of ligand-receptor pairs between specific cell types¹²⁰, and more recently also leveraging spatial information using graph neural networks¹²¹ (Figure 2). Sequencing physically interacting cells (PIC-seq) utilizes fluorescence-activated cell sorting to isolate physically interacting cells from dissociated tumors and assess crosstalk between neighboring cells using scRNA-seq¹²² (Figure 2). This overcomes the limitation of losing spatial organization due to tissue dissociation for scRNA-seq.^{37,38} (Figure 2,3). Spatial transcriptomics is another powerful technology to assess spatial gene expression without the need to digest tissue samples by using an array of spatial capture spots (barcoded oligos) across a tissue section¹²³. However, the currently used methods have several limitations, as they do not offer single-cell resolution but rather capture multiple cells on an individual capture barcode spot. To deconvolute distinct cell types, it is possible to integrate scRNA-seq data with spatial transcriptomics data and infer cell-type proportions¹¹¹. Moreover, the resolution of spatial transcriptomics datasets can be enhanced computationally by the recently developed BayesSpace toolkit, which subsets each capture barcode spot into multiple subspots¹²⁴. Integration of intracellular protein activity with scRNA-seq analysis can be used to identify specific functional subsets of different cell types with the intracellular staining and sequencing (INs-seq) integrated technology¹⁰⁹ (Figure 2), enabling investigation of signaling pathway activation, transcription factor expression or metabolic activity. INs-seq presents an approach with which to systematically investigate the molecular profile and signaling state of specific cell types of interest¹⁰⁹.

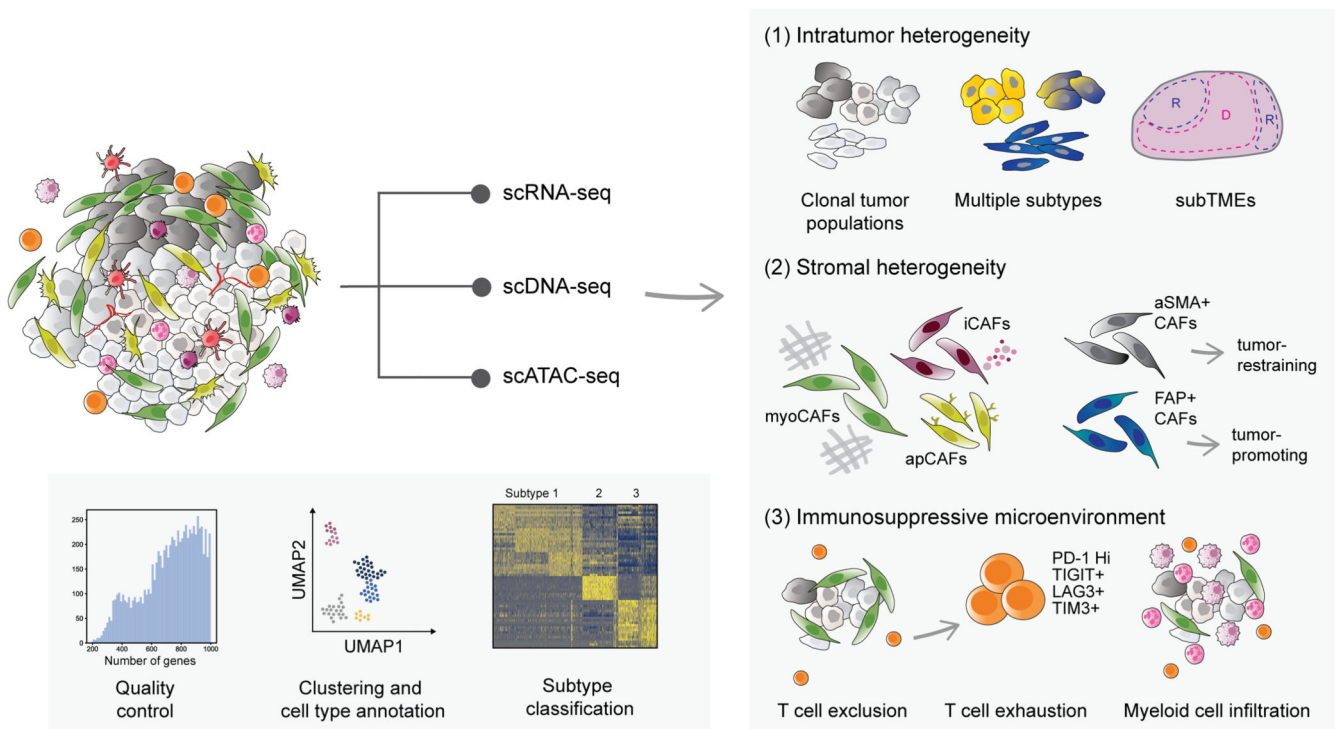


Figure 1. Single-cell profiling to uncover pancreatic cancer heterogeneity and complexity.

Left, single-cell profiling approaches, such as scRNA-seq (transcriptomics), scDNA-seq (genomics) and scATAC-seq (epigenetics), provide detailed insights into pancreatic cancer heterogeneity at various levels. Right, depicted are hallmarks of pancreatic cancer heterogeneity: (1) intratumor heterogeneity – tumors are composed of clonal tumor cell subpopulations, for which multiple tumor cell subtypes can co-occur within the same tumor, as well as diverse subTMEs, such as the deserted and reactive one; (2) stromal heterogeneity – the pancreatic cancer TME is characterized by a high abundance of CAF subsets (myoCAFs, iCAFs and apCAFs) with distinct functional phenotypes, for example, tumor-restraining (α SMA⁺ CAFs) and tumor-promoting (FAP⁺ CAFs) fibroblasts and (3) an immunosuppressive microenvironment – pancreatic cancer shows an exclusion of T cells or presence of exhausted, dysfunctional T cells, and tumors are highly infiltrated by immunosuppressive myeloid cells.

LAG3, lymphocyte-activation gene 3; PD-1, programmed cell death protein 1; TIM3, T cell immunoglobulin and mucin domain-containing protein 3; UMAP, uniform manifold approximation and projection.

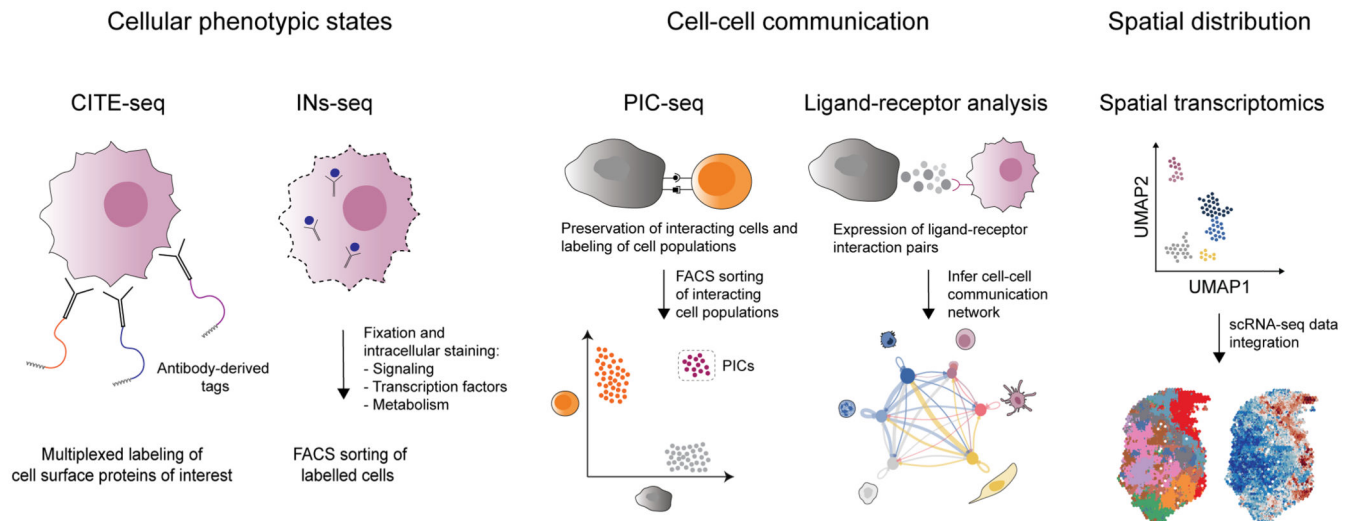


Figure 2. scRNA-seq approaches to decode cell-cell interaction and communication, as well as the spatial architecture of PDAC subtypes.

Left, using cellular indexing of transcriptomics and epitopes by sequencing (CITE-seq), the simultaneous expression of cell-surface protein markers, as well as gene expression, can be assessed. INs-seq enables the profiling of intracellular protein expression to infer signaling activity, transcription factor expression and metabolic states within single cells. Both approaches uncover distinct cellular phenotypic states. Middle, sequencing of physically interacting cells (PIC-seq) entails cell-cell communication analysis between two directly interacting cell subpopulations. Complex cell-cell communication networks are inferred by the expression of ligand-receptor interaction pairs of different cell types in the pancreatic cancer TME. Right, integration of scRNA-seq with spatial transcriptomics data allows analysis of spatial distribution and spatially resolved TME communities within a tumor. PIC, physically interacting cells.

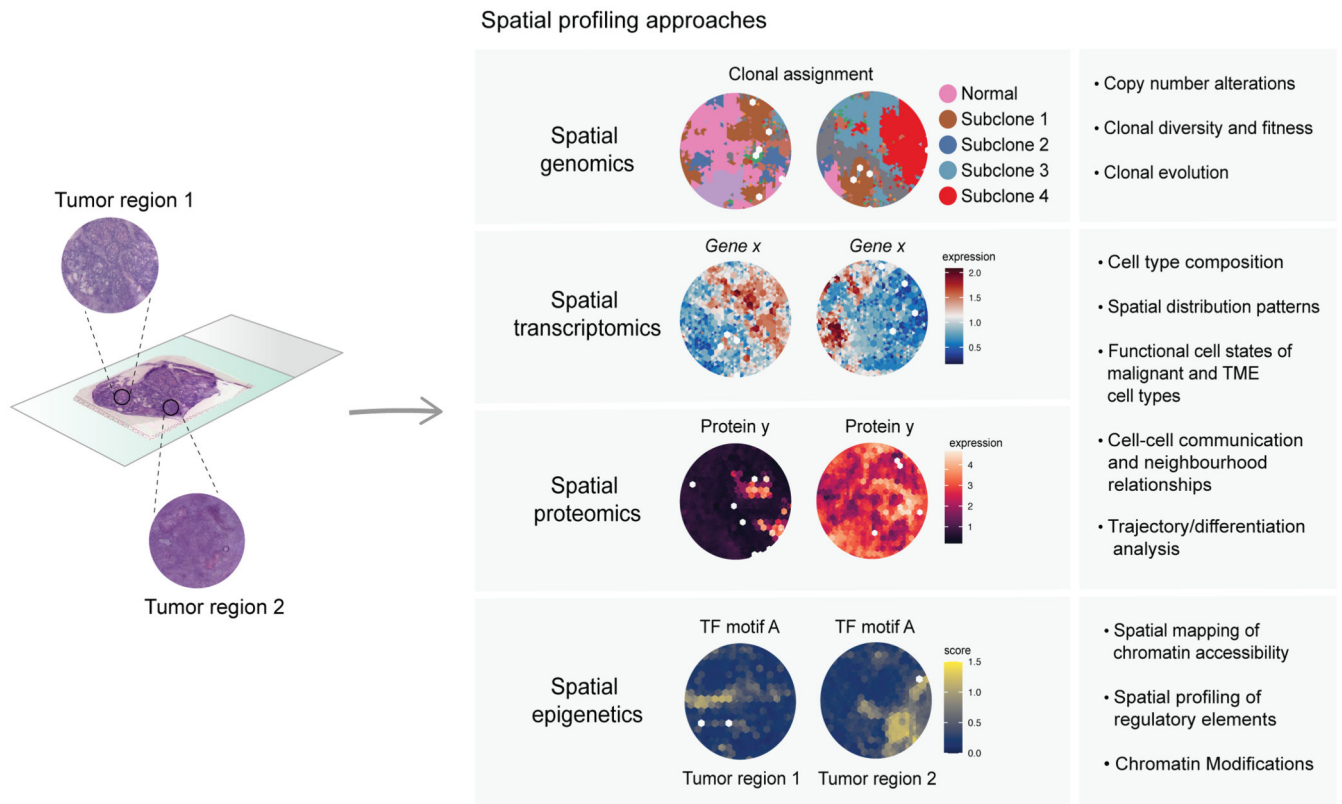


Figure 3. Multimodal spatial single-cell profiling technologies.

Overview of spatial profiling technologies encompassing spatial genomics, spatial transcriptomics, spatial proteomics and spatial epigenetics approaches to assess inter- and intratumor heterogeneity and the spatial organization of pancreatic cancer. Spatial profiling methods are applied to analyze intact tissue sections without the need to dissociate the tissue, thereby preserving the spatial architecture of the tumor. Spatial genomics (spatial DNA-seq) identify tumor cell subclones and reveal differences in spatially defined regions within the tumor. Using spatial transcriptomics and proteomics, different cell types and functional cell states can be assessed. Besides, cell-cell communication channels and networks between neighboring cell types can be analyzed in a spatially resolved manner. Spatial epigenetics approaches allow the profiling of chromatin accessibility and chromatin modifications in distinct tumor regions.

TF, transcription factor.

Table 1
Selected scRNA-seq analyses uncovering PDAC subtype and TME heterogeneity

Study	Cohort and sample type	Sample size	Single-cell platform	Subtype analysis	Biological insights/relevance
Ref. 58	<ul style="list-style-type: none"> Six primary human PDACs: two low-grade IPMNs, two high-grade IPMNs and two PDACs (resected) 	5,403 cells	SureCell WTA 3' for ddSEQ system	NA	<ul style="list-style-type: none"> Cellular heterogeneity during progression of cystic PDAC precursor lesions (IPMNs) to invasive cancer
Ref. 64	<ul style="list-style-type: none"> Three PDAC samples of early-KIC, late-KIC and late-KPFC mice One normal pancreas sample 	9,575 cells	3' scRNA-seq (10x Genomics), v2 chemistry	<ul style="list-style-type: none"> Classical Mesenchymal 	<ul style="list-style-type: none"> Cellular heterogeneity during tumor progression Mesenchymal tumor cells enriched in late-stage tumors
Ref. 66	<ul style="list-style-type: none"> 24 primary human PDAC (untreated) 11 normal human pancreas samples 	57,530 cells	3' scRNA-seq (10x Genomics), v2 chemistry	<ul style="list-style-type: none"> Squamous Immunogenic Progenitor ADEX 	<ul style="list-style-type: none"> Analysis of intratumor heterogeneity Characterization of ductal cell gene expression profiles
Ref. 93	<ul style="list-style-type: none"> PDAC:CAF co-culture model Human PDAC-3 line (GFP-Luc-tagged) Human CAF-1 cells (mCherry-tagged) 	92 PDAC cells and 92 CAF cells	SMARTseq (SMARTer Ultra Low Input v3 kit; Clontech)	<ul style="list-style-type: none"> Classical Quasi-mesenchymal 	<ul style="list-style-type: none"> Integration of scRNA-seq/RNA-ISH analysis with protein profiling (flow cytometry and CyTOF) Analysis of co-culture model of patient-derived PDAC and CAF cell line to understand effect of CAFs on tumor cell heterogeneity and characterize cell-cell interactions
Ref. 75	<ul style="list-style-type: none"> Six primary human PDACs (untreated) Two adjacent normal tissue samples Four mouse PDACs (KPC model) 	21,200 human PDAC cells and 11,260 mouse PDAC cells	3' scRNA-seq (10x Genomics), v2 chemistry	NA	<ul style="list-style-type: none"> Cellular heterogeneity of all cell types in PDAC Delineating fibroblast heterogeneity in a cross-species analysis Identification of novel CAF population described as apCAFs
Ref. 59	<ul style="list-style-type: none"> Nine mouse pancreas samples from PRT mice taken at different time 	41,139 mouse pancreas cells and 5,184 human PDAC cells	3' scRNA-seq (10x Genomics), v2 and v3 chemistry	NA	<ul style="list-style-type: none"> Time-point analysis of metaplastic acinar cell heterogeneity using a tamoxifen-inducible mouse model (<i>Ptf1a-CreER,LSL-</i>

Study	Cohort and sample type	Sample size	Single-cell platform	Subtype analysis	Biological insights/relevance
	<ul style="list-style-type: none"> points after tamoxifen injection One primary human PDAC sample 				<ul style="list-style-type: none"> <i>Kras^{G12D}, LSL-tdTomato</i> Cell interaction analysis between metaplastic cells and TME cell types
Ref. 7	<ul style="list-style-type: none"> 15 primary human PDAC samples (13 resected and two metastatic) 	31,195 cells	3' scRNA-seq (10x Genomics), v2 chemistry	<ul style="list-style-type: none"> Classical A Classical B Hybrid Basal-like A Basal-like B 	<ul style="list-style-type: none"> Novel PDAC subtype classification from purified PDAC epithelium Hybrid subtype: overlap of classical and basal-like gene expression Co-occurrence of classical and basal-like cells in the majority of samples
Ref. 84	<ul style="list-style-type: none"> Two normal pancreas samples from albino Bl6 mice (five mice per replicate) Two pancreas samples from KPP mice: adjacent normal tissue, small and large tumors (five mice per replicate) 	13,454 cells	3' scRNA-seq (10x Genomics)	NA	<ul style="list-style-type: none"> Analysis of fibroblast heterogeneity during tumor progression Optimized dissociation method to preserve PDPN⁺ fibroblasts for scRNA-seq analysis Identification of novel LRRC15⁺ CAFs exhibiting an immunosuppressive activity
Ref. 115	<ul style="list-style-type: none"> Six primary patient-derived PDAC organoids 	8,934 cells	SPLiT-seq	<ul style="list-style-type: none"> Classical Basal-like (mesenchymal) 	<ul style="list-style-type: none"> Intra-tumoral heterogeneity within classical tumor compartment Identification of basal-like tumor cells within classical PDAC organoids
Ref. 116	<ul style="list-style-type: none"> Ten primary human PDACs (resected) Six metastases (five liver and one omentum) from patients with metastatic PDAC biopsies) 	8,000 primary cells and 6,926 metastases	3' scRNA-seq (10x Genomics), v2 chemistry	<ul style="list-style-type: none"> Classical Progenitor Squamous Quasi-mesenchymal Basal 	<ul style="list-style-type: none"> Analysis of PDAC subtype signatures in distinct cell type compartments Correlative analysis of defined cell type signatures with patient survival High EMT tumor cell expression correlated with shorter survival Classical tumor cell expression not correlative of survival
Ref. 41	<ul style="list-style-type: none"> Two primary human 	1,926 PDAC-A cells and	inDrop	NA	<ul style="list-style-type: none"> Multimodal intersection analysis

Study	Cohort and sample type	Sample size	Single-cell platform	Subtype analysis	Biological insights/relevance
	PDACs (resected)	1,733 PDAC-B cells			<ul style="list-style-type: none"> by integrating scRNA-seq with spatial transcriptomics data Identification of unique cancer cell subpopulations and their spatial localization
Ref. 68	<ul style="list-style-type: none"> 16 primary human PDACs (untreated, resectable and unresectable) Three nonmalignant pancreas 16 patient-matched PBMC Four healthy PBMCs 	46,344 PDAC cells, 8,541 nonmalignant cells, 55,873 PDAC PBMCs and 14,240 healthy PBMCs	3' scRNA-seq (10x Genomics)	NA	<ul style="list-style-type: none"> Multimodal integration of scRNA-seq with CyTOF and multiplexed immunohistochemistry Inclusion of fine-needle biopsy samples, which present in patients with unresectable PDAC Characterization of immune TME landscape in treatment-naïve patients with PDAC
Ref. 65	<ul style="list-style-type: none"> Orthotopically implanted mouse PDACs: <i>KRAS</i>-intact and <i>KRAS</i>-knockout KPC tumors from two different experiments 	10,000 cells from all conditions pooled	3' scRNA-seq (10x Genomics), v2 chemistry	<ul style="list-style-type: none"> Classical Basal-like (mesenchymal) 	<ul style="list-style-type: none"> Ablation of <i>KRAS</i> in pancreatic cancer evokes antitumor immune response Loss of <i>KRAS</i> leads to changed immune cell infiltration (higher T/B cell infiltrates) and tumor cell phenotypes (change to basal-like subtype)
Ref. 55	<ul style="list-style-type: none"> 20 primary patient-derived PDAC organoids Four patient-derived metastasis organoids (matched liver, peritoneal and perivascular) 	93,096 cells	3' scRNA-seq (10x Genomics), v2 chemistry	<ul style="list-style-type: none"> Classical Basal-like (mesenchymal) 	<ul style="list-style-type: none"> Characterization of transcriptional PDAC subtypes in patient-derived organoids Organoids showed uniformly classical or heterogenous (including basal-like) gene expression Heterogenous phenotype correlative to poorer patient survival Drug screen performed on patient-derived organoid cohort revealed a better drug response of the classical subtype
Ref. 117	<ul style="list-style-type: none"> 13 normal human pancreas samples 	> 120,000 nuclei (snRNA-seq)	3' scRNA-seq (10x Genomics), v2 and v3 chemistry	NA	<ul style="list-style-type: none"> Characterization of human pancreas cell types Optimized protocol for nuclei isolation from normal pancreas

Study	Cohort and sample type	Sample size	Single-cell platform	Subtype analysis	Biological insights/relevance
					<ul style="list-style-type: none"> Identified distinct acinar cell populations
Ref. 85	<ul style="list-style-type: none"> Ten in vitro multiplexed (MULTI-seq) human pDAC-derived CAF cultures 	6,331 cells	3' scRNA-seq (10x Genomics), v3 chemistry	<ul style="list-style-type: none"> Classical Basal-like (mesenchymal) 	<ul style="list-style-type: none"> Identification of PDAC subTMEs (reactive versus deserted) Reactive subTME associated with basal-like state Classical subtype associated with deserted subTME
Ref. 53	<ul style="list-style-type: none"> 23 human metastatic PDACs and matched patient-derived organoids (19/23 samples from liver metastases, two samples from peritoneal metastases, one sample from omentum and one from adrenal gland metastases) 	7,740 malignant cells, 15,302 nonmalignant cells and 24,995 matched organoids	Seq-Well array	<ul style="list-style-type: none"> Classical Intermediate co-expressor Basal (mesenchymal) 	<ul style="list-style-type: none"> Assessment of PDAC subtype cancer cell states Identification of drivers of transcriptional plasticity Analysis of relationships between subtype-state and TME phenotype Benchmarking of subtype-specific phenotypes in patient-derived organoid models
Ref. 102	<ul style="list-style-type: none"> Nine primary and metastatic human PDACs (fine-needle and core biopsies) 	31,720 cells	3' scRNA-seq and 5' scRNA-seq (10x Genomics)	<ul style="list-style-type: none"> Classical Basal-like Hybrid 	<ul style="list-style-type: none"> Characterization of malignant and TME cell types Ligand-receptor interaction analysis between tumor cells and TME cell types identified potential cell-cell communication routes
Ref. 63	<ul style="list-style-type: none"> Orthotopically implanted mouse PDACs: three classical and three mesenchymal tumors (six libraries each) Treatment conditions: control, T/N and T/N+anti-PD-L1 	30,677 cells	3' scRNA-seq (10x Genomics), v3 chemistry	<ul style="list-style-type: none"> Classical Mesenchymal 	<ul style="list-style-type: none"> Analysis of treatment-induced effects on tumor and TME cells of novel combinatorial therapy in vivo in PDAC subtypes Mesenchymal subtype showed higher sensitivity and benefited from additional immunotherapy Integration of scRNA-seq with tumor cell secretomes to delineate treatment-induced tumor-immune crosstalk

Study	Cohort and sample type	Sample size	Single-cell platform	Subtype analysis	Biological insights/relevance
Ref. 56	<ul style="list-style-type: none"> Four primary human PDAC samples (Osaka University cohort) Integration of five publicly available scRNA-seq datasets 	NA	3' scRNA-seq (10x Genomics), v3.1 chemistry	<ul style="list-style-type: none"> Normal cells Both low Basal-like high Classical high Both high 	<ul style="list-style-type: none"> Integration of six human PDAC scRNA-seq datasets (five datasets were previously published) to build scRNA-seq reference atlas of human PDAC Refined clustering and annotation of tumor cell subtypes CAF subtype analysis and identification of tumor-CAF interactions
Ref. 78	<ul style="list-style-type: none"> Eight KPC mouse PDACs: early-stage (five libraries) and late-stage (three libraries) 	31,861 cells	3' scRNA-seq (10x Genomics), v2 chemistry	NA	<ul style="list-style-type: none"> Profiling of CAFs from early- and late-stage mouse PDAC (KPC model) Identification of <i>aSMA</i>⁺ and <i>Fap</i>⁺ CAF subpopulation with opposing functions and prognosis
Ref. 103	<ul style="list-style-type: none"> 33 primary human PDACs: MD-Anderson 1 cohort (enriched for CD3⁺ T cells) and MD-Anderson 2 cohort (all cells) 24 primary human PDACs (integrated from Peng et al.⁶⁶) 	39,694 cells	3' scRNA-seq and 5' scRNA-seq (10x Genomics)	NA	<ul style="list-style-type: none"> Analysis of functional T cell states in human PDAC samples Reference atlas of T cell subpopulations
Ref. 39	<ul style="list-style-type: none"> 43 primary human PDACs: 18 untreated and 25 treated with neoadjuvant therapy Single-cell nuclei sequencing performed (snRNA-seq) 	224,988 nuclei	3' scRNA-seq (10x Genomics), v2 and v3 chemistry	<ul style="list-style-type: none"> ACN CLS BSL SQM MES NEN NRP 	<ul style="list-style-type: none"> Analysis of treatment-associated changes in TME composition and cancer cell gene expression programs Refined taxonomy of cancer cell expression signatures and association of PDAC subtypes with clinical outcome Refined classification of CAF subtypes and definition of multicellular TME communities Integration of whole-transcriptome spatial digital profiling to identify the spatial distribution

Study	Cohort and sample type	Sample size	Single-cell platform	Subtype analysis	Biological insights/relevance
					and interaction of multicellular communities
Ref. 57	<ul style="list-style-type: none"> 83 primary human PDAC samples from 31 patients (21 patients treated with standard-of-care therapy, including four normal adjacent tissue samples and ten treatment-naive patients) scRNA-seq and snRNA-seq performed 	232,764 cells (scRNA-seq) 83,860 nuclei (snRNA-seq)	3' scRNA-seq (10x Genomics), v3 chemistry	<ul style="list-style-type: none"> Duct-like-1 Duct-like-2 Acinar tumor Acinar normal Acinar <i>REG⁺</i> PanIN PDAC 	<ul style="list-style-type: none"> Analysis of transitioning cancer cell populations (untreated and standard-of-care treated) in combination with matched spatial transcriptomics datasets Assessment of spatial heterogeneity in treated patients with PDAC Analysis of treatment-associated changes in TME composition and cancer cell gene expression programs Identification of distinct CAF subsets across treatment groups Enrichment of iCAFs in chemoresistant samples Characterization of myeloid and lymphocyte populations across treatment groups

ADEX, aberrantly differentiated endocrine exocrine; GFP, green fluorescent protein; IPMN, intraductal papillary mucinous neoplasm; KIC, *Kras^{LSL-G12D/+}Ink4a^{fl/fl}Ptf1a^{cre/+}*; KPC, *Kras^{LSL-G12D/+}Trp53^{LSL-R172H/+}Pdx1-cre*; KPfC, *Kras^{LSL-G12D/+}Trp53^{fl/fl}Pdx1-cre*; KPP, *Kras^{LSL-G12D/+}Cdkn2a^{fl/fl}Pdx1-cre*; LRRC15, leucine-rich repeat containing 15; Luc, luciferase; NA, not applicable; PanIN, pancreatic intraepithelial neoplasia; PBMC, peripheral blood mononuclear cell; PD-L1, programmed death-ligand 1; PDPN, podoplanin; PRT, *Ptf1a^{cre/+}Kras^{LSL-G12D/+}R26^{LSL-tdTomato}*; RNA-ISH, RNA in situ hybridization; T/N, trametinib/nintedanib.